Invariance of success probability in Grover's quantum search under local noise with memory

Sheikh Parvez Mandal [1,2] Ahana Ghoshal,[2] Chirag Srivastava [2] and Ujjwal Sen [2]

[1]*Indian Institute of Science Education and Research, Pune 411 008, India*
[2]*Harish-Chandra Research Institute, A CI of Homi Bhabha National Institute, Chhatnag Road, Jhunsi, Prayagraj 211 019, India*

We analyze the robustness of Grover's quantum search algorithm performed by a quantum register under a possibly time-correlated noise acting locally on the qubits. We model the noise as originating from an arbitrary but fixed unitary evolution U of some noisy qubits. The noise can occur with some probability in the interval between any pair of consecutive noiseless Grover evolutions. Although each run of the algorithm is a unitary process, the noise model leads to decoherence when all possible runs are considered. We derive a set of unitary U's, called good noises, for which the success probability of the algorithm at any given time remains unchanged with varying nontrivial total number m of noisy qubits in the register. The result holds irrespective of the presence of any time correlations in the noise. We show that only when U is either of the Pauli matrices σ_x and σ_z (which give rise to m-qubit bit-flip and phase-damping channels, respectively, in the time-correlation-less case), the algorithm's success probability stays unchanged when increasing or decreasing m. In contrast, when U is the Pauli matrix σ_y (giving rise to m-qubit bit-phase flip channel in the time-correlation-less case), the success probability at all times stays unaltered as long as the parity (even or odd) of the total number m remains the same. This asymmetry between the Pauli operators stems from the inherent symmetry-breaking existing within the Grover circuit. We further show that the positions of the noisy sites are irrelevant in the case of any of the Pauli noises. The results are illustrated in the cases of time-correlated and time-correlation-less noise. We find that the former case leads to a better performance of the noisy algorithm. We also discuss physical scenarios where our chosen noise model is of relevance.

I. INTRODUCTION

The past few decades have seen the advent and flourishing of the field of quantum information and computation. One of the most important classes of discoveries made in this field has to be that of quantum algorithms which provide or are believed to provide substantial computational advantages over their classical counterparts. The most significant ones include the Deutsch-Jozsa algorithm [1,2], Shor's factoring algorithm [3,4], the quantum search algorithms [5–10], and the quantum simulation algorithms [11–16]. The advantages of these quantum algorithms are assumed to be derived from the efficient use of quantum coherence and entanglement.

After Grover's seminal proposal [5,6] of his eponymous quantum search algorithm, which has been shown to be a special case of the more general amplitude amplification algorithm [17], an extensive amount of research effort has been directed towards implementing and studying the effect of noise on the efficiency of the algorithm in an actual quantum device. The experimental implementation of the algorithm was first done using nuclear magnetic resonance techniques [18]. Later on, the efficiency of Grover's algorithm was studied in [19] and a generalization of the algorithm for an arbitrary amplitude distribution was done in [8]. For more works on the applications of the quantum search algorithm see [20–28] and for some experimental implementations see [29–37].

Even if a quantum algorithm theoretically provides significantly better efficiency in comparison with its classical counterpart, the efficiency in an implementation of the same undoubtedly depends on the actual fabrication of the relevant quantum circuit. Due to possible impurities in circuit components and their erroneous implementations, fluctuations or drifts may arise, which can affect the performance of the quantum algorithm considerably. Therefore, characterizing such deviations from the ideal situation, caused by decoherence and noise, is important to assess the usefulness of an algorithm. The disturbances may cause a unitary noise on the ideal system, i.e., a small perturbation can arise in the Hamiltonians describing the unitary gates, conserving the Hermiticity of the Hamiltonian as well as the unitarity of the quantum gates (see, e.g., [38–41]).

Studies of the consequences of noisy scenarios in quantum algorithms started several decades back [42]. The effect of noise on the Grover search algorithm was studied in [43], which investigated the effect of random Gaussian noise on the algorithm's efficiency at each step. A perturbative method was used in [44] to study decoherence in a noisy Grover algorithm where each qubit suffers phase-flip error independently after each step. The effect of a noisy oracle was considered in [45,46]. In [47] the effect of depolarizing channels on all qubits was examined and it was found that the number of iterations needed to obtain the maximal efficiency of the success probability decreases with increasing decoherence. The effect of the Grover unitary becoming noisy was considered in [48] using a noisy Hadamard gate, with unbiased and isotropic noise, uncorrelated in each iteration of the Grover operators.

An upper bound on the strength of the noise parameters up to which the algorithm works efficiently was deduced. A comparison of the effects of several completely positive and trace-preserving maps on the efficiency and computational complexity of the algorithm was described in [49]. The performance of the algorithm under localized dephasing was studied in [50]. For more discussions and further ramifications of noise on Grover's algorithm, see [51–53]. A fault-ignorant quantum search was proposed in [54] where the searched element is reached eventually but with the runtime depending on the noise level. Steane's [55] quantum error correction code was also employed in the presence of the depolarizing channel in [56]. On the other hand, noise with correlations in time [57–69] and space [70–72] has been observed in realistic quantum computing devices and the detrimental effects of such noise on quantum error correcting codes have also been reported [73–77].

In this paper we study the effects of a noise that originates from the probabilistic noisy unitary evolution of some register qubits in between any two Grover operations. In particular, we find a set of noisy qubit unitaries, for which the success probability of the algorithm remains unaffected by the number of noisy qubits. We refer to those special noise unitaries as good noises. We extend our investigation to a type of time-correlated noise considered in [78–80] and examine its effects on the performance of the algorithm.

We have organized the paper as follows. After reviewing the noiseless Grover algorithm in Sec. II A, we introduce our noise model and its physical motivation in Sec. II B. The dynamics of the register under the Markovian-correlated noise is analyzed in Sec. II C. The time-correlation-less case of our noise model and its connection to some fundamental decoherence processes are then elucidated in Sec. II D. In Sec. III we give an overview of our analysis for finding the good noises. A measure of the algorithm's performance is introduced in Sec. IV A. The effects of a memoryless and of a Markovian-correlated noise on the efficiency of Grover's algorithm are numerically studied in Sec. IV B. Section V summarizes the paper.

II. GROVER SEARCH: THE NOISELESS CASE AND OUR NOISE MODEL

The Grover search algorithm that we consider here aims to find a single marked element from a search space of finite size. It is known to attain a quadratic speedup over the best classical search. In our paper we consider a Grover search under a time-correlated local noise. In the succeeding sections we discuss the ideal Grover algorithm and then introduce our noise model.

A. Noiseless scenario

The search algorithm is concerned with a search space $\{x\} = \{1, 2, \ldots, N\}$ with $N = 2^n$ elements. There exists a function $f : \{x\} \rightarrow \{0, 1\}$ defined such that

$$f(x) = \begin{cases} 1 & \text{for } x = w \text{ (marked element)} \\ 0 & \text{for } x \neq w. \end{cases} \quad (1)$$
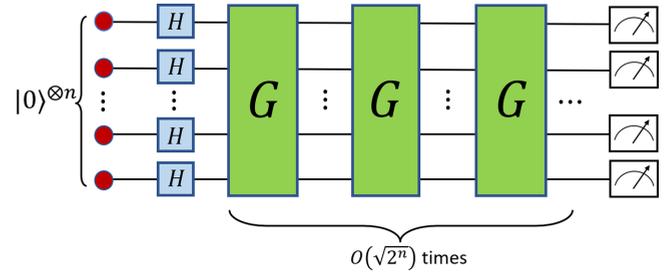

FIG. 1. Grover's search algorithm in the noiseless situation. The register containing a string of n qubits, each in the state $|0\rangle$, is subjected to a Hadamard operation in the first step. The second step is the operation of the Grover operator, for t times, which is followed by a measurement on the output state of the register in the computational basis. The time taken to reach the maximal success probability is $O(2^{n/2})$. See the text for further discussion.

To search for the marked element w, a classical computer evaluates f for each of the elements until the value 1, i.e., the marked element is found. This requires $O(N)$ operations. The advantage of Grover's search algorithm over the classical one is that, by using a sequence of unitary operations, it can find the marked element in only $O(\sqrt{N})$ queries to f. The steps of the algorithm are described as follows and a schematic demonstration is shown in Fig. 1.

It starts with all the qubits of an n-qubit register in the $|0\rangle$ state, where $|0\rangle$ is the eigenvector of a Pauli-z operator with eigenvalue 1. The next step is to act on each qubit by the Hadamard operator $H = \frac{1}{\sqrt{2}}(\sigma_x + \sigma_z)$, where σ_x and σ_z are Pauli operators. This takes the total register to a uniform superposition state

$$|s\rangle = \left(\frac{|0\rangle + |1\rangle}{\sqrt{2}}\right)^{\otimes n} = \frac{1}{\sqrt{N}}\left(\sum_{\substack{x=1 \\ x \neq w}}^{N} |x\rangle + |w\rangle\right), \quad (2)$$

where $|w\rangle$ is the marked state, i.e., the state corresponding to the element we are searching for in the database of $N = 2^n$ elements. The state $|s\rangle$ is then acted on by the Grover operator G, given by $G = DO$, where $D = (2|s\rangle\langle s| - \mathbb{1}_N)$ is called the diffuser and $O = (\mathbb{1}_N - 2|w\rangle\langle w|)$ is the oracle. (For a detailed discussion about the construction of the diffuser D, oracle O, and the Grover G unitaries, see, e.g., [41,81].) The operator G has the form

$$G = -\mathbb{1}_N + 2|s\rangle\langle s| - \frac{4}{\sqrt{N}}|s\rangle\langle w| + 2|w\rangle\langle w|. \quad (3)$$

It acts on successive states until the state of the register $|\psi(t)\rangle = G^t|s\rangle$ reaches close enough to the marked state $|w\rangle$. Here t stands for the number of times the Grover operator is employed after the first step, i.e., after the Hadamard operation. The success probability, i.e., the probability to find the marked state after the tth operation, is given as $P(t) = |\langle w|\psi(t)\rangle|^2$. It can be checked that the marked element is reached after around $t = \lfloor \frac{\pi}{4}\sqrt{N} \rfloor$ Grover iterations (see Fig. 2).
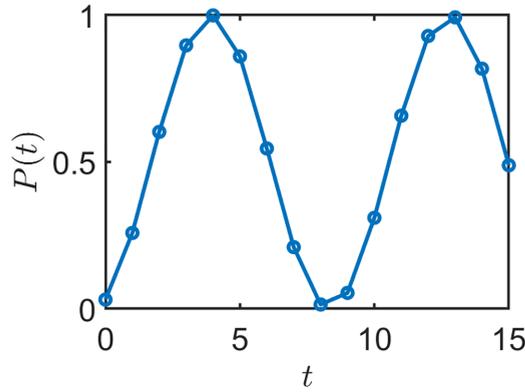
FIG. 2. Noiseless Grover algorithm for $n = 5$ qubits in the register. The number t of Grover iterations is along the horizontal axis and the success probability $P(t)$ for finding the marked state is plotted on the vertical axis. The smallest t for which $P(t)$ is maximal is given by $t = 4$. All quantities plotted are dimensionless.

B. Noise model

For a large database, the number of iterations of the Grover operator will be large, although quadratically smaller than that for the classical algorithm, to reach the first maximal success probability. A high number of applications of Grover operator may result in some noise or fluctuations in the circuit parameters performing the computation, affecting the efficiency of the algorithm [82,83]. In this paper we consider that in the interval between any two consecutive Grover operations, some m out of a total of n qubits evolve under some unitary U that we call the noise unitary, at a rate specified by the noise probability. Such local single-qubit errors in a quantum register due to probabilistic unitary qubit evolutions have been studied previously in numerous settings (see the discussions and references in Secs. I and II D).

We express the effect of this noisy evolution in the form of the total noise unitary χ_m acting on the whole register. For example, it can be $\chi_m = U \otimes (\mathbb{1}_2)^{\otimes(n-m)} \otimes U^{\otimes(m-1)}$, meaning m noisy qubits evolving under U and $n - m$ noiseless qubits acted on by the identity operator $\mathbb{1}_2$. We refer to the number of noisy qubits m as the noise strength. The positions of the m noise sites are allowed to be arbitrary, but are fixed during a given run of the algorithm. The noise χ_m occurs with some well-defined probability after every Grover iteration and we can incorporate its effect on the algorithm by defining a new unitary $G' = \chi_m G$, which we refer to as the noisy Grover operator. Using Eq. (3), we obtain

$$G' = -\chi_m + 2(\chi_m |s\rangle\langle s| + \chi_m |w\rangle\langle w|) - \frac{4}{\sqrt{N}} \chi_m |s\rangle\langle w|. \quad (4)$$

The probabilistic occurrences of the noise could possibly even be correlated in time and we assume in this paper that the noise at each consecutive time step is Markovian correlated.

The motivation behind choosing this type of noise model comes from the possibility of spatiotemporally correlated errors [84,85] and unwanted qubit crosstalk [86–90] in the currently available experimental setups for implementing the Grover search algorithm. We discuss below one such noisy scenario.
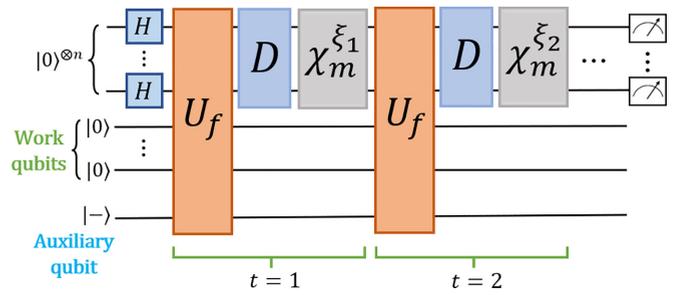

FIG. 3. Circuit diagram for the Grover algorithm under time-correlated noise. The n-qubit register is initialized in the state $|0\rangle^{\otimes n}$. The total noise unitary χ_m acts in between two consecutive perfect Grover iterations. Here ξ_t is the Markovian process introduced in Sec. II B 1, D denotes the diffuser unitary of Sec. II A, U_f implements the oracle O using the work and auxiliary qubits initialized in states $|0\rangle$ and $|-\rangle$, respectively, and t denotes the number of noisy Grover iterations.

1. Physical scenario motivating the noise model

Let us first discuss the ideal experimental setup of the implementation of Grover's search algorithm. We have already discussed in Sec. II A that the Grover operator G contains two parts: One is the diffuser D and the other is the oracle O. The ideal experimental setup can be seen in Fig. 3, if we ignore the noisy evolutions $\chi_m^{\xi_i}$ for $i = 1, 2, \ldots$. As shown in Fig. 3, the oracle O can be implemented by introducing an auxiliary qubit and an oracle workspace [41] to the circuit. The auxiliary qubit in this case needs to be initialized in the state $|-\rangle = \frac{|0\rangle - |1\rangle}{\sqrt{2}}$ and then evolved together with the quantum register, under the unitary U_f, that acts on the joint state of the register and auxiliary qubit $|x\rangle \otimes |q\rangle$ as follows:

$$U_f(|x\rangle \otimes |q\rangle) = |x\rangle \otimes |q \oplus f(x)\rangle. \quad (5)$$

Here the function $f(x)$ is given in Eq. (1) and $\oplus$ denotes the modulo 2 addition. It can be easily verified that $|q\rangle = |-\rangle$ recovers the oracle operation on the register's state so that $U_f(|x\rangle \otimes |-\rangle) = (O|x\rangle) \otimes |-\rangle$. The physical implementation of U_f generally requires the use of multiple work qubits [41,91,92] in the oracle workspace (see Fig. 3). Suppose the workspace has $\bar{n}$ work qubits, each initialized in state $|0\rangle$ and then evolved with the auxiliary and the n register qubits under some combination of several one-qubit and two-qubit gates, depending on the particular U_f [93]. The two-qubit gates, due to technical constraints [82,94–98] of physical implementation, require the concerned qubits to be in close proximity [99,100]. This increases the possibility of spatially correlated errors [84,85] on those qubits. Unwanted crosstalk [86–90] could creep in while the qubits are idle, i.e., in between any two Grover steps, when no gates are applied on the register. For these types of errors and noises, some of the register qubits face noisy evolutions.

Let us consider that between two Grover steps, a crosstalk error occurs due to a stochastic interaction Hamiltonian [101] of the form

$$\Theta^{(r,v)} = \xi_t \left(h^{(r)} \otimes \sigma_z^{(v)} \right), \quad (6)$$

with $h^{(r)}$ acting on the rth qubit of the register and the Pauli $\sigma_z^{(v)}$ acting on the vth work qubit. The dimensionless

coupling strength ξ_t undergoes fluctuations at each time step. The Hamiltonians $h^{(r)}$ and $\Theta^{(r,\nu)}$ are taken to be dimensionless. The Hamiltonian $h^{(r)}$ leads to the local noisy unitary $U = \exp(-ih^{(r)})$ on the register qubit at each time step, as described in Sec. II B. For the composite setup of the register and the auxiliary qubit, we have $\exp(-i\,\Theta^{(r,\nu)}) = U^{\xi_t} \otimes |0\rangle\langle 0| + (U^\dagger)^{\xi_t} \otimes |1\rangle\langle 1|$, which is a unitary on the rth register qubit controlled by the νth work qubit [102,103] at each time step.

Now suppose that any m of the total n-qubit register suffer the crosstalk error, given in Eq. (6), in the interval between two Grover iterations at time t. Hence, the total noisy Hamiltonian becomes $\Theta = \sum_{(r,\nu)} \Theta^{(r,\nu)}$, where the sum is over all the (r,ν) pairs corresponding to the m noisy register qubits. In the physical implementation of Grover's algorithm, all the work qubits are unitarily brought back to state $|0\rangle$ after each oracle operation using uncomputation [104–107]. Thus, the state of the workspace before and after the complete oracle operation is $|0\rangle^{\otimes n}$. So the joint state of the register $|\psi(t)\rangle$ and the oracle workspace evolve under the total noise unitary, due to the interaction Hamiltonian in Eq. (6), as $e^{-i\Theta}[|\psi(t)\rangle \otimes |0\rangle^{\otimes n}]$. This situation is analogous to the case where the noise unitary χ_m, introduced in Sec. II B, acts on the register qubits. Therefore, we can write

$$e^{-i\Theta}[|\psi(t)\rangle \otimes |0\rangle^{\otimes n}] = \left[\chi_m^{\xi_t}|\psi(t)\rangle\right] \otimes |0\rangle^{\otimes n}. \quad (7)$$

Here ξ_t indicates that the noise can be time correlated. The occurrence of this type of noise is demonstrated in Fig. 3.

In this paper we consider the coupling strength ξ_t to be a time-homogeneous discrete-time Markov process [108–110]. In particular, we choose the dichotomous Markov chain considered in [78–80,111]. This kind of time-dependent coupling strength may arise due to a noisy coupling field, which couples the register and work qubits [112–114], and also due to a qubit in the environment [115] or a spurious control field [116]. For our noise model, ξ_t takes the two values 0 and 1 according to the following conditional probabilities:

$$\Pr(\xi_{t+1} = l | \xi_t = k) = (1-\mu)\Pr(\xi_t = k) + \mu\delta_{lk}$$
$$= (1-\mu)p_k + \mu\delta_{lk} = p_{l|k}. \quad (8)$$

Here $p_k = \Pr(\xi_t = k)$ denotes the probability of the event k of the Markov process and $p_{k|l}$ denotes the conditional probability of event k, given that event l happened in the previous time step. The parameter μ will be referred to as the memory parameter and it can take any real value from 0 (memoryless) to 1 (perfect memory).

This kind of correlated noise with partial memory can potentially be found in real quantum devices and it has been shown to provide an enhancement in the transmission of classical information compared to transmission through noisy channels without memory [78]. In Sec. II C we describe the register's time evolution under this time-correlated noise. It will become evident that such a scenario could arise if the noisy qubits in the quantum register get coupled to an external degree of freedom acting as a physical memory state [103,117–119].
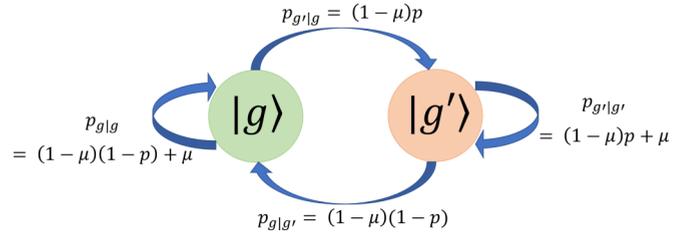

FIG. 4. Schematic diagram of transitions of the walker's state at $t \geqslant 2$ with the conditional probabilities defined in Eq. (8). See the text for details.

C. Time evolution under Markovian-correlated noise

In our noise model, a total unitary evolution by χ_m of locally evolving m noisy qubits is a probabilistic process, happening after each noiseless Grover evolution G. This noisy evolution is probabilistic in the sense that after a given Grover evolution G, the state of the register is a convex mixture of two possible states: one corresponding to no noise after evolution by G and another corresponding to a noisy evolution by χ_m after G. Now, as we discussed in Sec. II B, it can happen that the probability of noise at a given time depends on the history of the register's noisy evolution [120,121]. In this paper we consider the simplest of such situations, where this noise is Markovian correlated in time (see Appendix B). In this case, the evolution at each given instant is affected only by the immediately previous time step. This potentially important variety of noise with memory has not yet been studied before in the case of the Grover algorithm. It should be noted here that the results shown in the paper are not exclusive to only this kind of noise, and the validity in this case will serve as an indication of the generality of the results.

The time evolution under the time-correlated noise is easier to describe if we incorporate an extra (not necessarily physical) degree of freedom, the walker, which we can trace out after the evolution of the composite register-walker state. The walker helps to keep track of the fluctuating coupling strength ξ_t introduced in Sec. II B 1. The walker has two orthogonal states $|g\rangle$ and $|g'\rangle$ and at each time step it performs a transition between these two states with some well-defined probability. In particular, it is in the state $|g'\rangle$ when $\xi_t = 1$ and in $|g\rangle$ when $\xi_t = 0$. A schematic diagram is shown in Fig. 4. When it transitions to $|g'\rangle$, all the m qubits connected to it are rotated by a unitary U and the other $n - m$ are left as they were. When it transitions to $|g\rangle$, all the n qubits connected to it are left as they were. Thus, at each time step, application of an ideal unitary Grover operator G is followed by each of the following with some corresponding probabilities: (I) Any m out of n qubits are rotated by a unitary U, i.e., the walker is in state $|g'\rangle$, and (II) all the n qubits are left untouched, i.e., the walker is in state $|g\rangle$. To make the situation clearer, let us say that after the $(t-1)$th noisy Grover iteration, the register is in a state given by the density matrix ρ_{t-1}. After the noisy (t)th iteration, the register will be a convex mixture of the following two possible states:

$$\rho_t = G'\rho_{t-1}G'^\dagger \quad \text{with } G' = \chi_m G \quad \text{[Possibility (I)]},$$
$$\rho_t = G\rho_{t-1}G^\dagger \quad \text{[Possibility (II)]}.$$

These processes are dictated by the state of the walker, which in turn performs transitions according to the Markov process as described in Eq. (8). When $\mu = 0$, noise at each time step is independent of what happened in the previous step, since $p_{k|l} = p_k$. On the other hand, $\mu = 1$ leads to $p_{k|k} = 1$, meaning that in the case of perfect memory, the walker state remains fixed throughout the evolution. At $t = 1$, i.e., for the first Grover iteration, the probabilities of (I) and (II) are determined by the initial probabilities of the walker to be in states $|g'\rangle$ and $|g\rangle$, respectively. These probabilities are called stationary probabilities and are taken to be $p_{g'} = p$ and $p_g = 1 - p$, respectively. Here p can be referred to as the noise probability. Note that here p and $1 - p$ are equal to p_1 and p_0, respectively, in Eq. (8).

Before the application of the first Grover iteration, the n-qubit register is in the uniform superposition state corresponding to $\rho_0 := |s\rangle\langle s|$. Thus the density matrix of the composite system containing the walker and the register before applying the first Grover iteration is $R_0 = \left(\frac{|g\rangle + |g'\rangle}{\sqrt{2}}\right)\left(\frac{\langle g| + \langle g'|}{\sqrt{2}}\right) \otimes |s\rangle\langle s|$. So the state of the register after the first and subsequent Grover iterations will be obtained by tracing out the walker from R_t, i.e., $\rho_t = \mathrm{Tr}_{\text{walker}}\{R_t\}$. In the following, the superoperators $\Phi^g[\bullet]$ and $\Phi^{g'}[\bullet]$ acting on an operator ρ will represent unitary evolutions $G\rho G^\dagger$ and $G'\rho G'^\dagger$, respectively. The time evolution of ρ_t can then be expressed using transition operators S_0 and S as

$$\begin{aligned} R_1 = S_0 R_0 = &\{p_g(|g\rangle\langle g| + |g\rangle\langle g'|) \otimes \Phi^g[\bullet] \\ &+ p_{g'}(|g'\rangle\langle g| + |g'\rangle\langle g'|) \otimes \Phi^{g'}[\bullet]\}R_0 \\ = &\{p_g(|g\rangle\langle g| + |g\rangle\langle g'|) \otimes \Phi^g[\rho_0] \\ &+ p_{g'}(|g'\rangle\langle g| + |g'\rangle\langle g'|) \otimes \Phi^{g'}[\rho_0]\}. \end{aligned} \quad (9)$$

Therefore, $\rho_1 = \mathrm{Tr}_{\text{walker}}\{R_1\} = p_g \Phi^g[\rho_0] + p_{g'} \Phi^{g'}[\rho_0]$ and

$$\begin{aligned} R_2 = SR_1 = &(p_{g|g}|g\rangle\langle g| \otimes \Phi^g[\bullet] + p_{g|g'}|g\rangle\langle g'| \otimes \Phi^g[\bullet] \\ &+ p_{g'|g}|g'\rangle\langle g| \otimes \Phi^{g'}[\bullet] + p_{g'|g'}|g'\rangle\langle g'| \otimes \Phi^{g'}[\bullet])R_1. \end{aligned} \quad (10)$$

Hence, $\rho_2 = \mathrm{Tr}_{\text{walker}}\{R_2\} = \sum_{i,j} p_{i|j} p_j \Phi^i[\Phi^j[\rho_0]]$, where i and j can be g or g'. Similarly, for $t \geq 2$ we have

$$\begin{aligned} R_t &= S^{t-1}R_1, \\ \rho_t &= \mathrm{Tr}_{\text{walker}}\{R_t\}. \end{aligned} \quad (11)$$

The success probability, i.e., the probability to find the marked state at time t, is given as

$$P(t) = |\langle w|\rho_t|w\rangle|. \quad (12)$$

We show in Sec. II D that in the absence of any time correlations, our noise model reduces to some well-known decoherence processes.

D. Case of $\mu = 0$ and unital decoherence processes

In the case when the noise in consecutive steps does not have any time correlations, i.e., $\mu = 0$, Eq. (8) has the form $p_{g|g} = p_g = p_{g|g'}$ and $p_{g'|g} = p_{g'} = p_{g'|g'}$. Putting these in the expressions of S_0 and S, we get $S = S_0$. Taking the initial register state ρ_0 and the composite walker and register state

R_0 as given in Sec. II C, we get the register's state ρ_1 after the first noisy Grover iteration as

$$\begin{aligned} \rho_1 &= \mathrm{Tr}_{\text{walker}}\{R_1\} = \mathrm{Tr}_{\text{walker}}\{S_0 R_0\} \\ &= (1 - p)\Phi^g[\rho_0] + p\Phi^{g'}[\rho_0] \\ &= (1 - p)(G\rho_0 G^\dagger) + p\chi_m(G\rho_0 G^\dagger)\chi_m^\dagger. \end{aligned} \quad (13)$$

Thus, the noisy evolution after the first noiseless Grover operation is a quantum dynamical map [122–125] $\mathcal{E}$ given by the Kraus operators $K_1 = \sqrt{1 - p}\,\mathbb{1}_N$ and $K_2 = \sqrt{p}\,\chi_m$ so that $\mathcal{E}[\rho] = K_1\rho K_1^\dagger + K_2\rho K_2^\dagger$ and $\rho_1 = \mathcal{E}[G\rho_0 G^\dagger]$. Since $S_0 = S$ in the case of $\mu = 0$, we have, for $t \geq 1$,

$$\rho_t = \mathcal{E}[G\rho_{t-1}G^\dagger]. \quad (14)$$

Note that for $\mu > 0$, an expression like Eq. (14) is not possible because of noise being conditioned on the application at the previous time step.

For $U = \sigma_x$, the noisy operation $\mathcal{E}$ thus becomes an m-qubit bit-flip channel. Similarly, $U = \sigma_z$ leads to phase-damping and $U = \sigma_y$ to bit-phase-flip channels. A comparison of the effects of these channels on the Grover algorithm was done extensively in [49]. In fact, all these are examples of unital channels (that is, $\sum_i K_i^\dagger K_i = \mathbb{1}$) and *any* unital channel can be expressed, like in Eq. (13), as an affine combination of unitary channels [126].

We have shown how the memoryless special case of the Markovian-correlated noise gives rise to some of the most relevant sources of decoherence in quantum registers [87]. It is a general feature that the success probability of an algorithm decreases with an increase in the strength of noise, as seen, e.g., in [48], whereas there is a possibility of identifying such noise for which the decrease in the success probability does not depend on the number of noisy qubits m. (For an example, see Appendix A.) If it is possible to choose between different noise-generating unitaries in an experimental setup, it will be helpful to have those noise unitaries which do not decrease the success probability with an increase in the noise strength. We can refer to such noise unitaries as good noises. In the succeeding section, we try to identify the form of such good noises.

III. SET OF GOOD NOISES

To find what the good noises are, we will start with the most general single-qubit unitary matrix (in the $\{|0\rangle, |1\rangle\}$ basis), viz.,

$$U = \begin{pmatrix} a & b \\ -\bar{b}e^{i\theta} & \bar{a}e^{i\theta} \end{pmatrix}, \quad (15)$$

with $a, b \in \mathbb{C}$, $|a|^2 + |b|^2 = 1$, $\theta \in [0, 2\pi)$, and $\bar{z}$ denoting the complex conjugate of z. The good noise corresponds to the values of a, b, and θ, for which the success probability $P(t)$ [Eq. (12)] remains unchanged on changing the value of m. If the total noise unitary χ_m acts on m sites, we will denote $P(t)$ in that case by $P_m(t)$. The good noises will be found through elimination of U's for which $P_m(t)$ changes with m. We will also show the independence of the positions of the m noisy qubits as long as U is one of the Pauli matrices.

To start with, we will check under what conditions the success probability at time $t = 1$ remains constant under varying m. After that, we will extend our investigations for the times $t > 1$. A detailed calculation of the search for good noises is given in Appendix C for $t = 1$. The derivation begins with the aim to keep $P_m(t = 1) = (1 - p)|\langle w|G|s\rangle|^2 + p|\langle w|G'|s\rangle|^2$ constant with the alteration of m, and we find that both a and b of Eq. (15) cannot be nonzero [see the derivation of Eqs. (C3) and (C4)]. The first condition ('Condition-1') for constructing a good noise is $|a| = 1$ or $|b| = 1$. This condition implies that χ_m must be a generalized permutation unitary matrix. We can then introduce a state $|w'\rangle$ as follows:

$$\chi_m|w\rangle\langle w|\chi_m^\dagger = \begin{cases} |w\rangle\langle w| & \text{for } |a| = 1 \\ |w'\rangle\langle w'| & \text{for } |b| = 1. \end{cases} \quad (16)$$

It turns out that the state's evolution can be written in the basis $\mathbb{B}$, where

$$\mathbb{B} = \begin{cases} \{|s_1'\rangle, \dots, |s_M'\rangle, |w\rangle\} & \text{for } |a| = 1 \\ \{|s_1'\rangle, \dots, |s_M'\rangle, |w\rangle, |w'\rangle\} & \text{for } |b| = 1. \end{cases} \quad (17)$$

[See the arguments around Eqs. (C6) and (C7) in Appendix C.] The basis set $\mathbb{B}$ is different from the N-dimensional computational basis set $\{|x\rangle\}$ used in Eq. (2). The basis elements $|s_i'\rangle$ are constructed using the computation basis states $\{|d\rangle_i\}_{d\in\{x\}}$ as

$$|s_i'\rangle = \frac{1}{\sqrt{\Delta_i}} \sum_{|w\rangle, |w'\rangle \notin \{|d\rangle_i\}} |d\rangle_i,$$

with $\Delta_i = \mathcal{S}(\{|d\rangle_i\})$ (where $\mathcal{S}$ denotes cardinality of the set), $\bigsqcup_i \{|d\rangle_i\} = \{|x\rangle\}$, and $\langle s_i'|s_j'\rangle = \delta_{ij}$. The dimension of $\mathbb{B}$ is $M + 1$ and $M + 2$ for $|a| = 1$ and $|b| = 1$, respectively. For a matrix U satisfying 'Condition-1', there are two possibilities: Its two nonzero elements are either equal or unequal. As elaborated in Appendix C, this implies that

$$\dim(\mathbb{B}) = \begin{cases} 2 \text{ or } 3 & \text{for } |a| = 1 \\ 3 \text{ or } 4 & \text{for } |b| = 1, \end{cases} \quad (18)$$

which then leads to another necessary condition, 'Condition-2': $M = 1$ or 2. This requirement ensures that the dimension of the basis $\mathbb{B}$ remains constant for any given number of noise sites m (see Appendix C for more details). Conditions 1 and 2 narrow down the possible set of good noises to a restricted set of unitaries, the Pauli matrices $e^{i\phi}\mathbb{1}_2$, $e^{i\phi}\sigma_x$, $e^{i\phi}\sigma_y$, and $e^{i\phi}\sigma_z$ for any $\phi \in [0, 2\pi)$. Basically, we have derived that the above three (excluding the trivial $\mathbb{1}_2$) noises lead to $P_m(t = 1) = P_{m+1}(t = 1) \forall m$, thus satisfying the criteria for being good noises.

We now check if these noise unitaries belong to the set of good noises for all times, i.e., for $t > 1$. From Eqs. (9), (10), and (12) we can see that the success probability at time t, for m noisy qubits, can be written as $P_m(t) = \sum_{\{\gamma_m(t)\}} p_{\gamma_m(t)}|\langle w|\gamma_m(t)|s\rangle|^2$. Here $\{\gamma_m(t)\}$ is the set of results from the multiplication of all possible length-t configurations composed of the two unitaries G and G'. For example, at $t = 2$, $\{\gamma_m(2)\} = \{GG, GG', G'G, G'G'\}$. The $\{p_{\gamma_m(t)}\}$ are the respective probabilities of each such trajectory $\gamma_m(t)$ in $\{\gamma_m(t)\}$. To satisfy the requirement of $P_m(t) = P_{m+1}(t) \forall m$ and all t, we need to have $|\langle w|\gamma_m(t)|s\rangle| = |\langle w|\gamma_{m+1}(t)|s\rangle| \forall m$ for any

time t. We can check that $\langle w|\gamma_m(t)|s\rangle$ have to be polynomials of order t of the four variables: $\langle s|\chi_m|s\rangle$, $\langle s|\chi_m|w\rangle$, $\langle w|\chi_m|s\rangle$, and $\langle w|\chi_m|w\rangle$. Now, for $U \in \{\sigma_x, \sigma_y, \sigma_z\}$, we have $\chi_m^2 = \mathbb{1}_N$. So the constituent nonzero terms in $\langle w|\gamma_m(\tau)|s\rangle$ for any $t = \tau$ will have degrees with the same parity as τ, i.e., the degrees of each term will belong to the set $\{\tau, \tau - 2, \tau - 4, \dots\}$. For example, a trajectory $\gamma_m(2) = G'G'$ will correspond to the polynomial $\langle w|\gamma_m(2)|s\rangle$ of order 2. It contains terms of degree 2, such as $\langle w|\chi_m|s\rangle\langle s|\chi_m|s\rangle$ and $\langle w|\chi_m|w\rangle^2$, and terms of degree 0, such as $\langle w|w\rangle = 1$ and $\langle w|s\rangle = \frac{1}{\sqrt{N}}$.

It can be shown that $\langle s|\chi_m|s\rangle = \frac{1}{N}\sum_{k=1}^N \psi_q = [\frac{a+b}{2} + e^{i\theta}\frac{a-b}{2}]^m$, with ψ_q introduced in Eq. (C2). Also, $|\langle s|\chi_m|w\rangle| = |\langle w|\chi_m|s\rangle| = \frac{1}{\sqrt{N}}$ and $|\langle w|\chi_m|w\rangle| = |a|^m$. These results will be used in the following arguments for verifying the constancy of $|\langle w|\gamma_m(t)|s\rangle|$ with respect to m for any given t, in the case of the Pauli matrices.

For $U = \sigma_x$, we have $a = 0$, $b = 1$, and $\theta = \pi$. So $\langle s|\chi_m|s\rangle = 1$, $\langle w|\chi_m|s\rangle = \frac{1}{\sqrt{N}} = \langle s|\chi_m|w\rangle$, and $\langle w|\chi_m|w\rangle = 0 \forall m$. Thus, $|\langle w|\gamma_m(t)|s\rangle|$ for any t does not depend on m. This in turn implies that that $P_m(t)$ is independent of m in the case of $U = \sigma_x$.

For $U = \sigma_z$, we have $b = 0$, $a = 1$, and $\theta = \pi$ and so $\langle s|\chi_m|s\rangle = 0$. From Eq. (16) we have that the magnitudes $|\langle w|\chi_m|s\rangle|$, $|\langle w|\chi_m|w\rangle|$, and $|\langle s|\chi_m|w\rangle|$ remain constant with respect to m. Moreover, $\text{sgn}(\langle w|\chi_m|s\rangle) = \text{sgn}(\langle w|\chi_m|w\rangle) = \text{sgn}(\langle s|\chi_m|w\rangle) \forall m$, where $\text{sgn}(z) = \frac{z}{|z|}$ with $z \in \mathbb{R}$. Thus, in the case of σ_z, $|\langle w|\gamma_m(t)|s\rangle|$ for any t depends on the three variables $\langle w|\chi_m|s\rangle$, $\langle w|\chi_m|w\rangle$, and $\langle s|\chi_m|w\rangle$. The magnitudes of these variables remain constant with m, but their signs, which do vary with m, are nevertheless equal among themselves. We have shown above that the constituent terms of the polynomials are of the same parity (all even or all odd), whereby we can infer that the value of $|\langle w|\gamma_m(t)|s\rangle|$ is not affected by m. Hence, our claim for σ_z to be a good noise thus also holds for any time t.

In the case of $U = \sigma_y$, we have $a = 0$, $b = -i$, and $\theta = \pi$. So $\langle s|\chi_m|s\rangle = 0$ and $\langle w|\chi_m|w\rangle = 0$. We also have $\langle w|\chi_m|s\rangle = (-1)^m\langle s|\chi_m|w\rangle$. Thus, $|\langle w|\gamma_m(t)|s\rangle|$ for any t depends only on $\langle s|\chi_m|w\rangle$ and $(-1)^m$. For example, one of the elements of $\{\gamma_m(2)\}$ in the case of $P_m(2)$ is (GG'), for which $|\langle w|GG'|s\rangle|^2 = \frac{1}{N}|(1 - \frac{4}{N})^2 + \frac{4}{N}(-1)^m|^2$. Because of the presence of the $(-1)^m$ factor in some of the terms of any polynomial $|\langle w|\gamma_m|s\rangle|$ for $U = \sigma_y$, we can infer that the success probabilities $P_m(t) = P_{m+2}(t) \forall m$. That is, the success probability at any given time is not constant for all m's like in the case of σ_x or σ_z; instead, m's of equal parity have the same success probability among themselves at any given time.

So, for example, if we have a total of $n = 50$ qubits in the register performing the search algorithm, it turns out that the evaluation of the success probability in the case of $m = 22$ noise sites and that in the case of $m = 41$ noise sites will be indistinguishable if the qubits in those sites evolve under the good noises, i.e., $U \in \{\sigma_x, \sigma_z\}$. The success probabilities in the cases where $m = 10, 40$, or 50 will be exactly the same in the case of $U = \sigma_y$. Similarly, the cases of $m = 9, 33$, or 45 will be indistinguishable among themselves when $U = \sigma_y$. It should be noted that there may be some unitary U, other than these Pauli matrices, which makes the success probability independent of m for some particular time t and not at other
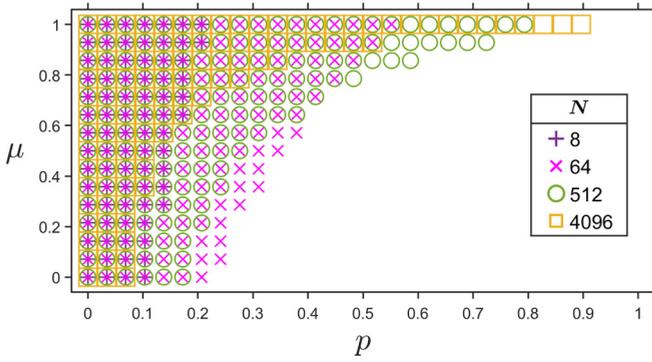
FIG. 5. Regime of memory parameter and noise probability for which the noisy Grover algorithm is at least as good (measured by the quantity $\tilde{P}$) as the classical search algorithm. The different colored symbols represent different sizes N of the search space. We find that the quantum search can withstand more noise if μ is higher. The advantage of the quantum algorithm becomes more evident with increasing N. All the quantities plotted are dimensionless.

times. The Pauli matrices σ_x and σ_z are special in the sense that when U is one of these, the success probability becomes independent of m for all t.
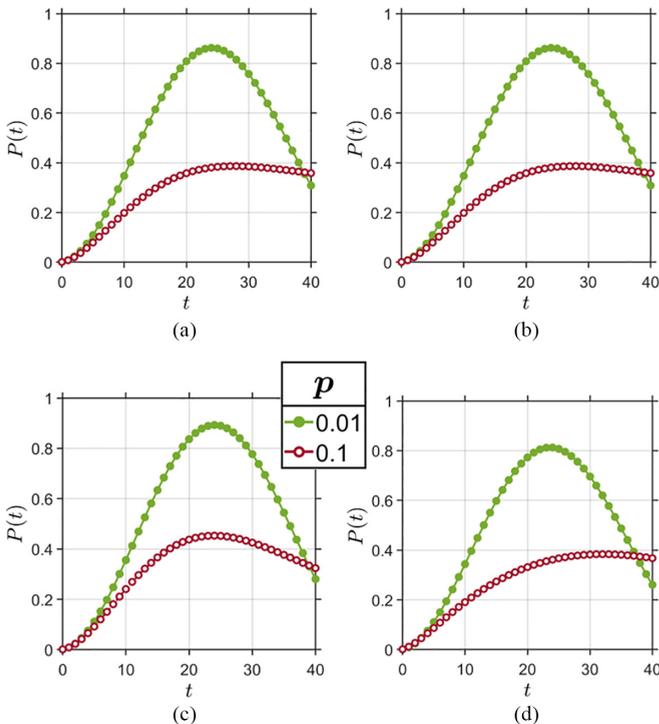

FIG. 6. Success probabilities of the Grover search algorithm in the presence of noise without any time correlation, i.e., $\mu = 0$. We have plotted $P(t)$ on the vertical axis and the number t of Grover steps along the horizontal axis for (a) $U = \sigma_x$ and $m = 1$, (b) $U = \sigma_x$ and $m = 5$, (c) $U = \frac{\sigma_x + \sigma_z}{\sqrt{2}}$ and $m = 1$, and (d) $U = \frac{\sigma_x + \sigma_z}{\sqrt{2}}$ and $m = 5$. The noise occurs with probability p at each Grover step. The plots are for a ten-qubit register with m noisy qubits (details are in Sec. IV B 1). The legend shows the symbols used in the plots for the noise probability p: 0.01 (closed green circles) and 0.1 (open brown circles). All quantities used are dimensionless.
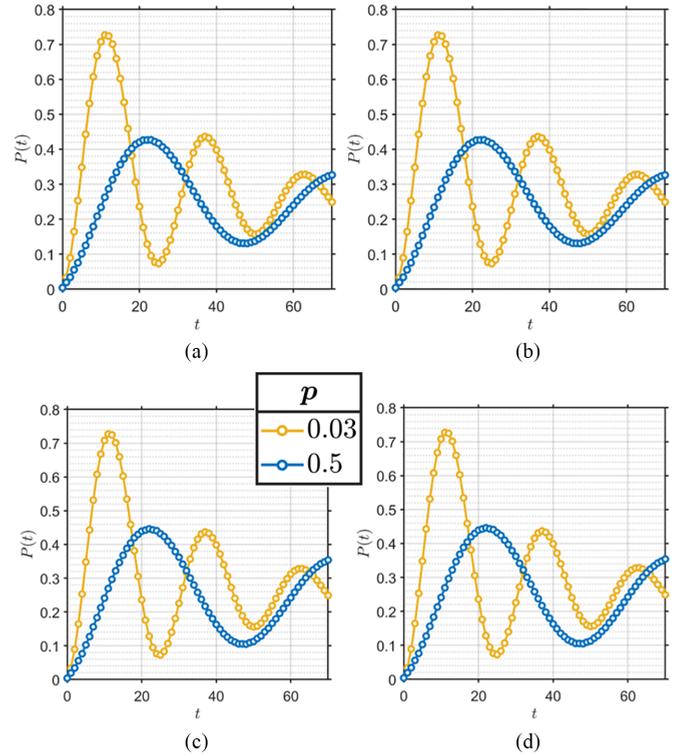

FIG. 7. Success probabilities of the Grover algorithm in the presence of noise without any time correlation, i.e., $\mu = 0$. We have plotted $P(t)$ on the vertical axis and the number t of Grover steps along the horizontal axis for $n = 8$, $U = \sigma_y$ (details in Sec. IV B 1), and noise strengths (a) $m = 1$, (b) $m = 5$, (c) $m = 2$, and (d) $m = 4$. The legend shows the symbols used for the noise probability p: 0.03 [yellow (light) curve] and 0.5 [blue (dark) curve]. As expected, the first maximum of $P(t)$ is higher in the case of the lower noise probability $p = 0.03$. All quantities used are dimensionless.

Another important observation is that none of the conditions used above put restrictions on what the positions of the m unitaries are, out of the total n positions. The coefficients c_i [in Eqs. (C6) and (C7)] remain the same for any arrangement of the m noisy qubits. So the success probability does not depend on the positions of the qubits which evolve under the noise unitary $U \in \{\sigma_x, \sigma_y, \sigma_z\}$. This result is also supported by Fig. 9. We will now investigate the effects of Markovian-correlated noise on Grover's search algorithm numerically; the results are gathered in the following section.

IV. EXAMPLES

Before numerically showing the invariance of success probabilities proved in the preceding section in the presence of the good noises, we will first identify the parameter regime in our noise model for which the algorithm performs better than classical search.

A. Performance of the noisy algorithm

The preservation of success probability upon increasing the number of noise sites is a potentially important feature. Nevertheless, increasing the noise probability still has a detrimental effect on the performance of the algorithm, as will be
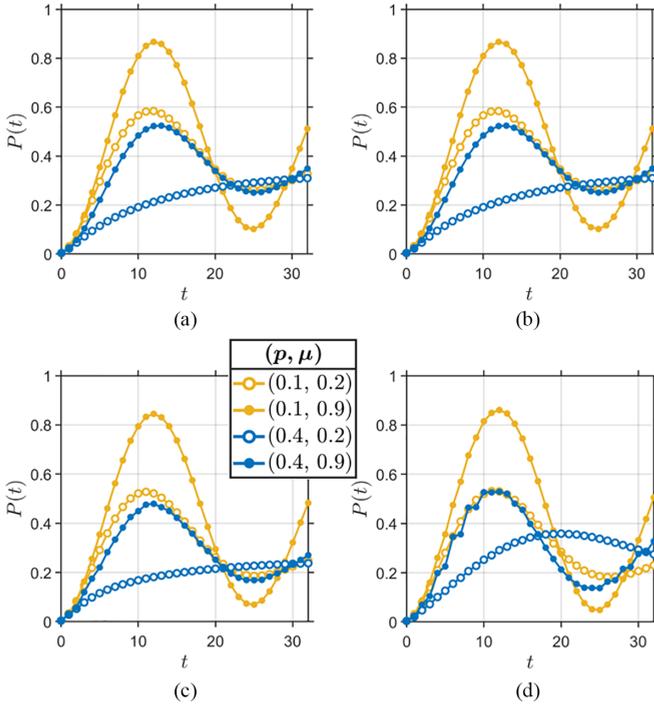
FIG. 8. Success probabilities of Grover's search algorithm in the presence of time-correlated noise. We have plotted $P(t)$ on the vertical axis and the number t of Grover steps along the horizontal axis for (a) $U = \sigma_x$ and $m = 1$, (b) $U = \sigma_x$ and $m = 4$, (c) $U = \frac{\sigma_y + \sigma_z}{\sqrt{2}}$ and $m = 1$, and (d) $U = \frac{\sigma_y + \sigma_z}{\sqrt{2}}$ and $m = 4$. The plots are for a register with $n = 8$ qubits, out of which m are noisy. The legend exhibits symbols used in the plots for different pairs of values of the noise probability p and memory parameter μ: $p = 0.1$ [yellow (light) curve], $p = 0.4$ [blue (dark) curve], $\mu = 0.2$ (open circles), and $\mu = 0.9$ (closed circles). All quantities used are dimensionless.

evident in the analysis in Sec. IV B. Since the probability of finding the marked element in Grover's algorithm is given by a success probability which never reaches unity in the noisy scenario, the algorithm needs to be rerun multiple times to find the element with some confidence [43,49].

Suppose that a noisy register, searching for a marked state out of a total of N states, reaches its success probability maximum P at time T. A classical search would find the element in $\frac{N}{2}$ time steps on average. Thus, assuming $T < \frac{N}{2}$, the quantum algorithm reaches its global maximum approximately $q = \frac{N}{2T}$ times faster than the classical one. However, it being likely that P is much less than 1 for a noisy algorithm, we can claim that the quantum algorithm is at least as good as the classical one only if, after running the noisy algorithm q times, the probability $\tilde{P} = 1 - (1 - P)^q$ of finding the marked element at least once is close to unity. Here we take a probability of 0.95 to be the lower bound of such confidence.

In Fig. 5 we show the values of μ and p for which the register, under $U = \sigma_x$ noise, searching from a collection of N elements is at least as good as the classical algorithm. We can see that a higher memory μ helps the algorithm to perform better than its classical counterpart up to much higher noise probabilities. Another observation from the figure is that the

quantum advantage becomes more prominent in the case of larger database sizes N.

B. Patterns of success probability

In this section we first show that the invariance of the success probabilities in the case of Pauli noise unitaries persists irrespective of any time correlation in the noise. Then the independence from positions of the noise sites in the case of the good noises and the effect of memory on the algorithm are shown numerically.

1. Noise without memory

The case of $\mu = 0$, discussed in Sec. II D, is a noise without any memory or time correlation. So at each time step, the probability for the Grover operation to become noisy is $p_{g'} = p$. In Fig. 6 we compare the behavior in the case of two noise unitaries U. The noise sites are the first m qubits in the register, i.e., $\chi_m = U^{\otimes m} \otimes \mathbb{1}_2^{\otimes(10-m)}$.

The case of $U = \sigma_x$ here corresponds to an m-qubit bit-flip channel, as was shown in Sec. II D. We see that the success probability's evolution $P(t)$ for a given noise probability p is unchanged when the number of noisy qubits is increased from $m = 1$ to $m = 5$ for $U = \sigma_x$. We contrast this with the evolution of $P(t)$ in the case of $U = (\sigma_x + \sigma_z)/\sqrt{2}$, i.e., the Hadamard operator. This U is a linear combination of two Pauli matrices and thus is not a good noise. The $P(t)$ in the presence of this noise changes when the number of noise sites is increased from $m = 1$ to $m = 5$, as expected.

We have also plotted in Fig. 7 the success probability's evolution for $m = 1, 2, 4, 5$ in the presence of noise unitary $U = \sigma_y$ and $\mu = 0$, on an eight-qubit register. In other words, the register is under an m-qubit bit-phase-flip channel occurring with probability p after each noiseless Grover operation. As discussed in Sec. III, the behavior of $P(t)$, for any given p and n, is exactly the same for an odd number of total noise sites, i.e., for $m = 1$ and 5 in the figure. The same is true among noise strengths of even parity, $m = 2$ and 4. In Fig. 9, we will also see that the locations of the noisy qubits are not important in the case of the good noises $U = \sigma_x$, σ_y, or σ_y. In the next section we study how the success probability evolution is affected by the presence of time correlations in the noise.

2. Noise with finite time correlation

In Fig. 8 the success probability $P(t)$ of Grover's search algorithm for nonzero (positive) memory μ and for $n = 8$ qubits (256 elements in the search database) for two different noise unitaries is depicted. Here we have used the form of noise as $\chi_m = \mathbb{1}_2^{\otimes(8-m)} \otimes U^{\otimes m}$ with $m = 1$ and 4. We can observe that the success probability $P(t)$ depends on the noise probability p and the memory parameter μ. It is obvious that the success probability decreases with increasing noise probability, and we can see from all four panels that for a very high noise probability, the oscillatory behavior of $P(t)$ tends to vanish. It can be seen from Figs. 8(a) and 8(b) that for a good noise $U = \sigma_x$, $P(t)$ for a given p and μ remains unaffected when we change the number of noise sites m on which U is applied, whereas for a unitary $U = (\sigma_y + \sigma_z)/\sqrt{2}$,
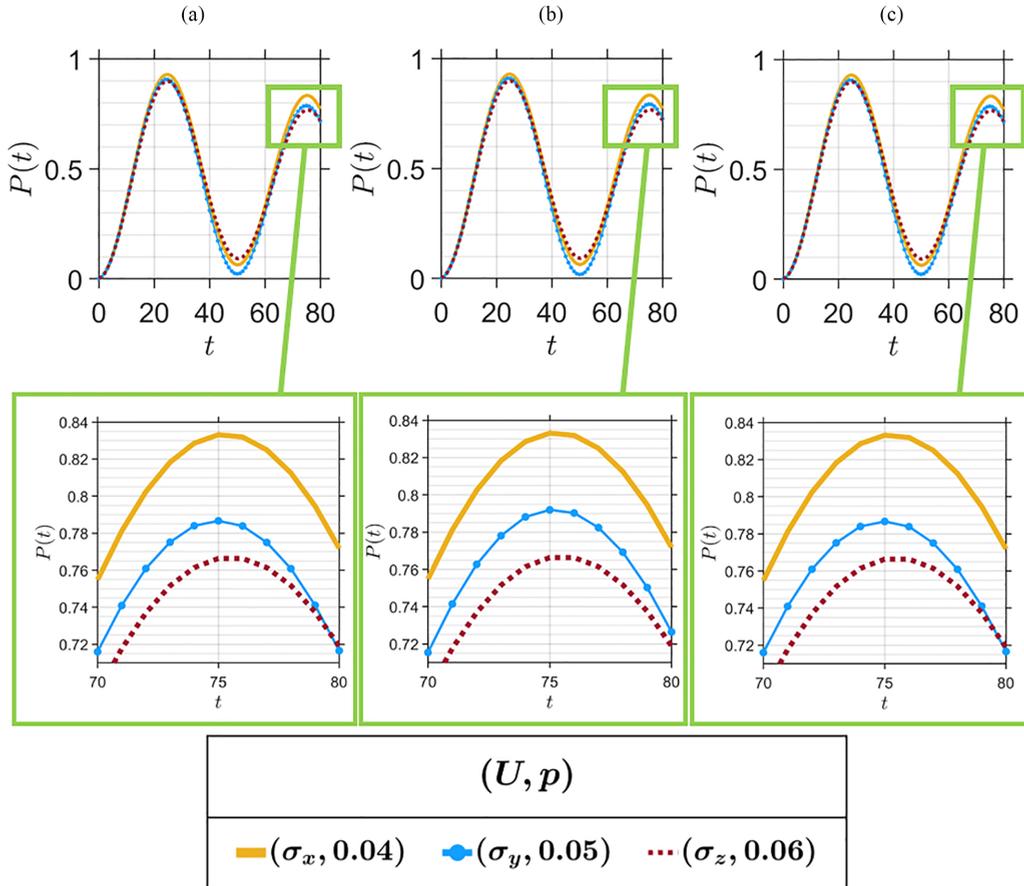
FIG. 9. Success probabilities of Grover algorithm for good noises. Here $n = 10$ and $\mu = 0.9$. Each of the colored curves is for a different p value and noise unitary U, as shown in the legend. The noise matrices χ_m are (a) $\chi_3 = U \otimes \mathbb{1}^{\otimes 7} \otimes U^{\otimes 2}$, (b) $\chi_{10} = U^{\otimes 10} \otimes U^{\otimes 2}$, and (c) $\chi_3 = \mathbb{1}^{\otimes 5} \otimes U^{\otimes 3} \otimes \mathbb{1}^{\otimes 2}$. The plots inside the green boxes show magnified views of the indicated smaller portions of the plots above. The total number of noisy qubits in (a) and (c) is $m = 3$, and in (b) $m = 10$. For $U = \sigma_y$, its corresponding curve (blue solid line with dots) in (b) is slightly different from those in the case of $U = \sigma_y$ in (a) and (c). This supports our claim that $P(t)$ in the case of $U = \sigma_y$ depends on the parity of m, unlike the other two Pauli matrices. All quantities used are dimensionless.

which was shown not to be a good noise before, the success probability $P(t)$ changes with the noise strength m. From a comparison of Figs. 8(c) and 8(d) we can see that in the case of a noise with low memory $\mu = 0.2$ and a high noise probability $p = 0.4$, the success probability evolution of the algorithm almost disappears. The noisy Grover search algorithm achieves greater efficiency for lower values of p and higher values of μ. Moreover, for higher values of p for which the oscillation of $P(t)$ completely vanishes, the correlated noise helps in achieving higher success probabilities. For example, compare the lines corresponding to $(p, \mu) = (0.4, 0.2)$ and $(0.4, 0.9)$ in the figure. The time evolution for $U = \sigma_x$ in the case of perfect memory ($\mu = 1$) is analyzed in Appendix D.

The success probabilities for the good noises are plotted with respect to time in Fig. 9 for different locations and numbers of noise sites. As we have noted previously in Sec. III, the positions of the noisy qubits do not matter if U is a good noise; however, it was also shown that the parity of the total number of noise sites is important in the case of $U = \sigma_y$. In Figs. 9(a) and 9(c) the parities of the total number m of noise sites are the same. Only the positions of the noise sites are different. As expected, the respective profiles of $P(t)$ in the case of all three

Pauli matrices are exactly the same in Figs. 9(a) and 9(c). In Fig. 9(b) all the qubits in the register are noisy and $m = 10$ is an even number; the behavior of $P(t)$ in the case of σ_y is not exactly the same as in Figs. 9(a) and 9(c), where m is odd for both. In contrast, $P(t)$ in the case of $U = \sigma_x$ and σ_z remains unaltered in Figs. 9(a)–9(c).

Figure 10 gives an overview of the effects of memory, database size, and noise probability on the algorithm's success. Here we plot the success probabilities at their first maxima $P(t = t^*)$ with respect to the noise probability p for $U = \sigma_x$. The effect of memory is contrasted in the three plots. As observed in Fig. 8, here also we can see that for a given amount of noise probability p, a higher memory μ of the noise helps the noisy algorithm reach a higher success probability.

V. CONCLUSION

Grover's algorithm can be employed to achieve a quadratic speedup over classical methods in an unstructured search. While this gives an advantage, a practical quantum circuit will undoubtedly be affected by different types of noise and several studies have already been pursued on the effects of
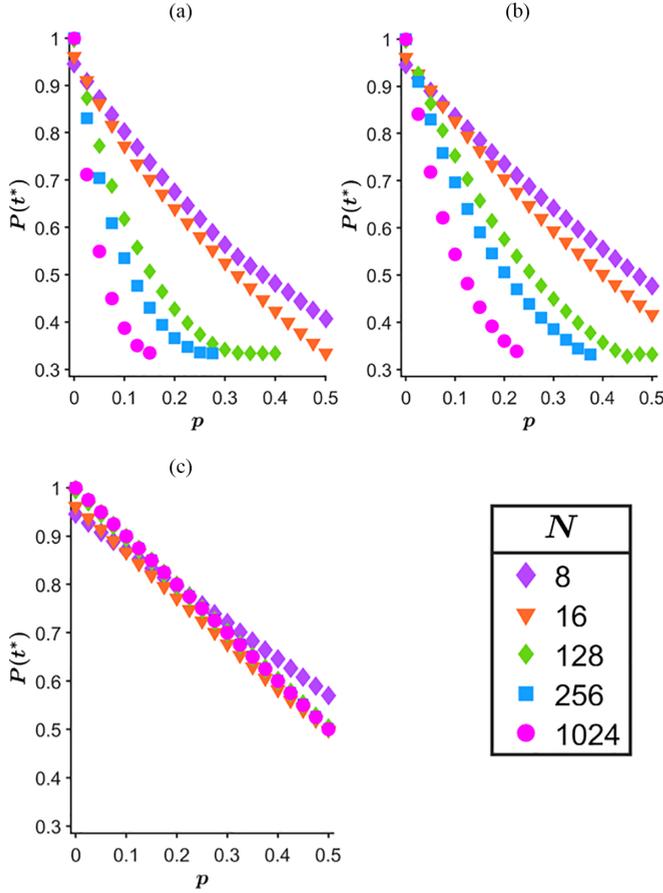
FIG. 10. Effects of memory, database size, and noise probability on the algorithm's success probability. We have presented here the values of $P(t^*)$, with respect to the noise probability p, for different (a) $\mu = 0$, (b) $\mu = 0.5$, and (c) $\mu = 1$. The algorithm is performed on $n = \log_2 N$ qubits. Here the noise unitary considered is $U = \sigma_x$. All quantities used are dimensionless.

such noises on the algorithm's performance. In our study, we considered the quantum register performing the algorithm to be under a local unitary noise which can also be correlated in time. In the interval between any two Grover operations, there is some probability for the noise to act on the register. In this setting, we found that the success probability of the algorithm at all times remains unchanged with respect to the number of noisy qubits if and only if the local noisy evolutions are given by some special unitaries. We refer to these unitaries as good noises. These noises have been shown to reduce to multiqubit bit-flip or phase-damping errors and in some cases bit-phase-flip errors in the absence of time correlations. The locations of the noisy qubits were also shown to be irrelevant in the case of the good noises. This can be potentially useful information in an actual implementation of the search algorithm on a register. The result that two of the Pauli noises behave in a different way than the third can be explained by the symmetry breaking in Grover's algorithm due to the choice of initial state of the algorithm's register (which is a product of eigenvectors of the Pauli σ_z operator) and the ensuing Hadamard rotation (which connects the σ_x and σ_z eigenbases). Numerically, we were also able to show that a time-correlated noise could lead to a better performance of the noisy algorithm.

APPENDIX A: SPECIAL CASE OF INVARIANCE OF SUCCESS PROBABILITY WITH RESPECT TO NOISE STRENGTH

In the case of $U = \sigma_x$, we get $\chi_m |s\rangle = |s\rangle$. So we can express all the states in terms of the orthogonal basis vector set $\{|s_1'\rangle, |w\rangle, |w'\rangle\}$, with $|s_1'\rangle = \frac{1}{\sqrt{N-2}} \sum_{x \neq w, w'} |x\rangle$.

In this basis, $\langle s| = \left(\sqrt{\frac{N-2}{N}} \quad \frac{1}{\sqrt{N}} \quad \frac{1}{\sqrt{N}} \right)$. From Eqs. (3) and (4) we obtain

$$G = \begin{pmatrix} 2\frac{N-2}{N} - 1 & -2\frac{\sqrt{N-2}}{N} & 2\frac{\sqrt{N-2}}{N} \\ 2\frac{\sqrt{N-2}}{N} & -\frac{2}{N} + 1 & \frac{2}{N} \\ 2\frac{\sqrt{N-2}}{N} & -\frac{2}{N} & \frac{2}{N} - 1 \end{pmatrix}, \quad (A1)$$

$$G' = \begin{pmatrix} 2\frac{N-2}{N} - 1 & -2\frac{\sqrt{N-2}}{N} & 2\frac{\sqrt{N-2}}{N} \\ 2\frac{\sqrt{N-2}}{N} & -\frac{2}{N} & \frac{2}{N} - 1 \\ 2\frac{\sqrt{N-2}}{N} & -\frac{2}{N} + 1 & \frac{2}{N} \end{pmatrix}. \quad (A2)$$

It is evident from the expressions above that, at least for the case $U = \sigma_x$, although changing m changes the forms of the basis vectors $|w'\rangle$ and $|s_1'\rangle$ in the computational basis, elements of all the states or operators like $|s\rangle$ or G' remain the same in the $\{|s_1'\rangle, |w\rangle, |w'\rangle\}$ basis. Thus, increasing or decreasing the number m of noise sites does not affect the success probability (12) of the algorithm in the case of $U = \sigma_x$ and $m \geqslant 1$.

APPENDIX B: EXAMPLE OF A MARKOVIAN CORRELATED CHANNEL

An important example of noise with memory is the Markovian correlated Pauli channel investigated in [78–80]. In that paper they studied the classical capacity of channels with partial memory. More specifically, they considered a channel that applies π rotations along random sets of axes $l_1, l_2, \ldots, l_n$ on a sequence of n qubits, with joint probability $p_{l_1 l_2 \cdots l_n}$, where $\sum_{l_1, l_2, \ldots, l_n} p_{l_1 l_2 \cdots l_n} = 1$. They also assumed that the rotation about axes $l_1, \ldots, l_n$ form a Markov chain so that

$$p_{l_1 \cdots l_n} = p_{l_1} p_{l_2 | l_1} \cdots p_{l_n | l_{n-1}}, \quad (B1)$$

where $p_{i|j}$ denotes the conditional probability of rotation about the i axis given that the previous one was about the j axis. The conditional probabilities are given as

$$p_{i|j} = (1 - \mu) p_i + \mu \delta_{i,j}. \quad (B2)$$

Here μ corresponds to the relaxation time or memory. For example, if $\mu = 1$, the same rotation axis l_1 is used at all subsequent rotations, i.e., $l_1 l_1 \cdots l_1$ on the qubits.

APPENDIX C: DETAILS OF CALCULATION FOR $P_m(t = 1)$ OF SEC. III

In connection to the search for good noises, we detail here the conditions on U for keeping $P_m(t = 1) = (1 - p)|\langle w|G|s\rangle|^2 + p|\langle w|G'|s\rangle|^2$ constant with changing m. We have

$$
|\langle w|G'|s\rangle|^2 = \left|\left(1 - \frac{4}{N}\right)\langle w|\chi_m|s\rangle + \frac{2}{\sqrt{N}}\langle w|\chi_m|w\rangle\right|^2
$$
$$
= \frac{1}{N}\left|\left(1 - \frac{4}{N}\right)\sum_{j=1}^{N}(\chi_m)_{w,j} + 2(\chi_m)_{w,w}\right|^2,
$$
(C1)

where

$$
\chi_m|s\rangle = \frac{1}{\sqrt{N}}\begin{pmatrix}\sum_{j=1}^{N}(\chi_m)_{1,j}\\ \vdots \\ \sum_{j=1}^{N}(\chi_m)_{N,j}\end{pmatrix}.
$$

It can be shown that

$$
\sum_{j=1}^{N}(\chi_m)_{k,j} = e^{iq\theta}(a+b)^{m-q}(\bar{a}-\bar{b})^q := \psi_q
$$
(C2)

and $(\chi_m)_{k,k} = e^{iq\theta}a^{m-q}\bar{a}^q$, where $q \in [0, m]$ and q depends on k. Here each ψ_q appears $\left(\frac{N}{2^m}\right)\binom{m}{q}$ times in $\chi_m|s\rangle$. Since $|\langle w|G|s\rangle|^2$ is independent of m, we can conclude from the expression of $|\langle w|G'|s\rangle|^2$ in Eq. (C1) that to get $P_{m+1}(1) = P_m(1)$ we need either $|a| = 0$ or $|b| = 0$. Therefore, we get our first condition for constructing a good noise, which gives the constraints (C3) and (C4). So a good noise needs to obey 'Condition-1', i.e., $|a| = 1$ or $|b| = 1$. Thus

$$
U = \begin{cases}\begin{pmatrix} a & 0 \\ 0 & \bar{a}e^{i\theta}\end{pmatrix} & \text{for} \quad |a| = 1 \quad (C3)\\[2ex] \begin{pmatrix} 0 & b \\ -\bar{b}e^{i\theta} & 0\end{pmatrix} & \text{for} \quad |b| = 1. \quad (C4)\end{cases}
$$

Hence χ_m has to be a generalized permutation unitary matrix. We can now define a new state $|w'\rangle$ so that

$$
\chi_m|w\rangle\langle w|\chi_m^\dagger = \begin{cases}|w\rangle\langle w| & \text{for } |a| = 1 \\ |w'\rangle\langle w'| & \text{for } |b| = 1.\end{cases}
$$
(C5)

Using this we can write

$$
\chi_m|s\rangle = \frac{1}{\sqrt{N}}\begin{cases}\left(\sum_{i=1}^{M}c_i\sqrt{\Delta_i}|s_i'\rangle + \alpha|w\rangle\right) & \text{for } |a| = 1 \\[1ex] & (C6)\\[1ex] \left(\sum_{i=1}^{M}c_i\sqrt{\Delta_i}|s_i'\rangle + \alpha|w\rangle + \beta|w'\rangle\right) & \text{for } |b| = 1,\end{cases}
$$
(C7)

where

$$
|s_i'\rangle = \frac{1}{\sqrt{\Delta_i}}\sum_{\{|d\rangle_i\}\neq|w\rangle,|w'\rangle}|d_i\rangle,
$$

$\Delta_i = \mathcal{S}(\{|d\rangle_i\})$, $\bigsqcup_i\{|d\rangle_i\} = \{|x\rangle\}$, $\langle s_i'|s_j'\rangle = \delta_{ij}$, and $|c_i| = 1 = |\alpha| = |\beta|$, i.e., we get the basis $\mathbb{B} = \{|s_1'\rangle, |s_2'\rangle, \ldots, |s_M'\rangle, |w\rangle\}$ of dimension $M + 1$ from Eq. (C6) and $\mathbb{B} = \{|s_1'\rangle, |s_2'\rangle, \ldots, |s_M'\rangle, |w\rangle, |w'\rangle\}$ of dimension $M + 2$ from Eq. (C7).

Now there are two possibilities for a unitary U of the form in Eqs. (C3) and (C4): Its two nonzero elements are either equal [case (i)] or unequal [case (ii)]. Case (i) suggests that $M = 1$ and directly leads to the constraints, given in Eqs. (C8) and (C9), which have to be satisfied by U to be a good noise. In case (ii) we need to put further restrictions on U for the success probability to stay conserved with m. We should not have $\dim(\mathbb{B})$ changing with m. Thus, the number of distinct c_i's in Eqs. (C6) and (C7) must remain constant with m. There is total of M of these coefficients for both $|a| = 1$ and $|b| = 1$. For $m = 1$, e.g., for $\chi_1 = U \otimes \mathbb{1}_{N/2}$ in case (ii), there are only two distinct nonzero elements in χ_1, because U has two distinct nonzero elements. This implies that $M = 2$. Since M should remain constant with m, case (ii) leads to the conditions given in Eqs. (C10)–(C12). To summarize, we have the necessary (but not sufficient) condition ('Condition-2') for U to be a good noise, i.e., $M = 1$ or 2. Thus

$$
\chi_m|s\rangle = \begin{cases}c\left(\sqrt{\frac{N-1}{N}}|s_1'\rangle + \frac{1}{\sqrt{N}}|w\rangle\right) & \text{for } |a| = 1,\ M = 1 & (C8)\\[2ex] c\left(\sqrt{\frac{N-2}{N}}|s_1'\rangle + \frac{1}{\sqrt{N}}|w\rangle + \frac{1}{\sqrt{N}}|w'\rangle\right) & \text{for } |b| = 1,\ M = 1,& (C9)\end{cases}
$$

$$
\chi_m|s\rangle = \begin{cases}c_1\left(\sqrt{\frac{N-2}{2N}}|s_1'\rangle + \frac{1}{\sqrt{N}}|w\rangle\right) + \frac{c_2}{\sqrt{2}}|s_2'\rangle & \text{for } |a| = 1,\ M = 2 & (C10)\\[2ex] c_1\left(\sqrt{\frac{N-4}{2N}}|s_1'\rangle + \frac{1}{\sqrt{N}}|w\rangle + \frac{1}{\sqrt{N}}|w'\rangle\right) + \frac{c_2}{\sqrt{2}}|s_2'\rangle & \text{for } |b| = 1,\ M = 2,\ \alpha = \beta & (C11)\\[2ex] c_1\left(\sqrt{\frac{N-2}{2N}}|s_1'\rangle + \frac{1}{\sqrt{N}}|w\rangle\right) + c_2\left(\sqrt{\frac{N-2}{2N}}|s_2'\rangle + \frac{1}{\sqrt{N}}|w'\rangle\right) & \text{for } |b| = 1,\ M = 2,\ \alpha \neq \beta. & (C12)\end{cases}
$$

So only the U's that satisfy one of Eqs. (C8)–(C12) are the unitaries corresponding to the good noise for which $P(t)$ does not depend on the number of noise sites m. It can be shown that ψ_q appears $\left(\frac{N}{2^m}\right)\binom{m}{q}$ times in the column vector $\chi_m|s\rangle$. We have the following observations.

(i) If U satisfies Eq. (C8), then $b = 0$ and $\psi_q = c \, \forall \, q$. Solving for a and θ gives $a = e^{i\phi} = \sqrt[m]{c}$ and $\theta = 2\phi$, i.e., $U = \sqrt[m]{c} \begin{pmatrix} 1 & 0 \\ 0 & 1 \end{pmatrix} = \sqrt[m]{c} \, \mathbb{1}_2$.

(ii) If U satisfies Eq. (C10), then it turns out that we need (a) $\psi_q = \psi_{q+2} = c_1 \, \forall \, q$ even and (b) $\psi_q = \psi_{q+2} = c_2 \, \forall \, q$ odd. That is because $\binom{m}{0} + \binom{m}{2} + \binom{m}{4} + \cdots = \binom{m}{1} + \binom{m}{3} + \binom{m}{5} + \cdots = 2^{m-1}$, i.e., the sum of multiplicities of elements in $\chi_m |s\rangle$ from the set $\{\psi_q \mid q \text{ even}\}$ is equal to that in the case of elements from the set $\{\psi_q \mid q \text{ odd}\}$. Since $c_1 \neq c_2$, solving (a) and (b) for a and θ gives the solution $a = \sqrt[m]{c_1}$ and $\theta = 2\phi - \pi$. The solution corresponds to $c_1 = -c_2$, i.e., $U = \sqrt[m]{c} \begin{pmatrix} 1 & 0 \\ 0 & -1 \end{pmatrix} = \sqrt[m]{c} \, \sigma_z$.

(iii) If U satisfies Eq. (C9), then $a = 0$ and $\psi_q = c \, \forall \, q$. Solving for b and θ gives $b = e^{i\phi} = \sqrt[m]{c}$ and $\theta = 2\phi - \pi$, i.e., $U = \sqrt[m]{c} \begin{pmatrix} 0 & 1 \\ 1 & 0 \end{pmatrix} = \sqrt[m]{c} \, \sigma_x$.

(iv) If U satisfies Eq. (C11) or (C12), an analysis similar to the above can be performed and the solution is $U = \sqrt[m]{c} \begin{pmatrix} 0 & 1 \\ -1 & 0 \end{pmatrix} = \sqrt[m]{c} \, i\sigma_y$.

Here $\sqrt[m]{c}$ is only a constant phase factor. We can see from the above discussion for $P_m(t = 1)$ that the candidates for good noise are the unitaries $e^{i\phi} \mathbb{1}_2$, $e^{i\phi} \sigma_x$, $e^{i\phi} \sigma_y$, and $e^{i\phi} \sigma_z$ for any $\phi \in [0, 2\pi)$.

APPENDIX D: EVOLUTION OF SUCCESS PROBABILITY FOR PERFECT MEMORY FOR $U = \sigma_x$

Here we consider the case when $\mu = 1$, i.e., perfect memory. On the first noisy iteration (i.e., $t = 1$), G occurs with probability $1 - p$ and G' with p. Let us assume that, at $t = 1$, G is applied. Due to perfect memory, for all $t \geqslant 2$, the same operator G will be applied. This scenario corresponds to an ideal noiseless Grover algorithm. The success probability in this case will be denoted by $P(t)$ and the marked state is reached at $t \approx \frac{\pi}{4}\sqrt{N}$ [41].

If G' is applied at $t = 1$, for $t \geqslant 2$ the state of the whole n-qubit register would be $|\psi(t)\rangle = G'^t |s\rangle$. Using the form of G' in Eq. (A2) for $U = \sigma_x$,

$$\langle w | G'^t | s \rangle = \frac{(-1)^{t+1}}{\sqrt{N}} \text{Im}\left\{ \left[\tan\left(\frac{\theta}{2} \right) - i \right] e^{it\theta} \right\},$$

where $\theta = \cos^{-1}(\frac{2}{N})$ and $\text{Im}\{\bullet\}$ denotes the imaginary part of a complex number. Then the success probability at time t in this case is

$$P'(t) = |\langle w | G'^t | s \rangle|^2 = \frac{\cos^2(\theta t)}{N} \left[\tan\left(\frac{\theta}{2} \right) \tan(\theta t) - 1 \right]^2. \tag{D1}$$

Combining the above two cases, the success probability of a noisy algorithm at time t, with noise probability p and perfect memory $\mu = 1$, then becomes $(1 - p)P(t) + pP'(t)$.

[1] D. Deutsch and R. Jozsa, Rapid solution of problems by quantum computation, Proc. R. Soc. London Ser. A **439**, 553 (1992).

[2] D. Deutsch and R. Penrose, Quantum theory, the Church-Turing principle and the universal quantum computer, Proc. R. Soc. London Ser. A **400**, 97 (1985).

[3] P. Shor, in *Proceedings 35th Annual Symposium on Foundations of Computer Science* (IEEE, Piscataway, 1994), pp. 124–134.

[4] A. Ekert and R. Jozsa, Quantum computation and Shor's factoring algorithm, Rev. Mod. Phys. **68**, 733 (1996).

[5] L. K. Grover, in *Proceedings of the Twenty-Eighth Annual ACM Symposium on Theory of Computing* (Association for Computing Machinery, New York, 1996), pp. 212–219.

[6] L. K. Grover, Quantum Mechanics Helps in Searching for a Needle in a Haystack, Phys. Rev. Lett. **79**, 325 (1997).

[7] M. Boyer, G. Brassard, P. Høyer, and A. Tapp, Tight bounds on quantum searching, Fortschr. Phys. **46**, 493 (1998).

[8] E. Biham, O. Biham, D. Biron, M. Grassl, and D. A. Lidar, Grover's quantum search algorithm for an arbitrary initial amplitude distribution, Phys. Rev. A **60**, 2742 (1999).

[9] N. Shenvi, J. Kempe, and K. B. Whaley, Quantum random-walk search algorithm, Phys. Rev. A **67**, 052307 (2003).

[10] A. Ambainis, J. Kempe, and A. Rivosh, in *Proceedings of the Sixteenth Annual ACM-SIAM Symposium on Discrete Algorithms* (Society for Industrial and Applied Mathematics, Philadelphia, 2005), pp. 1099–1108.

[11] Y. Manin, *Computable and Uncomputable* (Sovetskoye Radio, Moscow, 1980).

[12] R. Feynman, Simulating physics with computers, Int. J. Theor Phys. **21**, 467 (1982).

[13] S. Lloyd, Universal quantum simulators, Science **273**, 1073 (1996).

[14] H. Bernien, S. Schwartz, A. Keesling, H. Levine, A. Omran, H. Pichler, S. Choi, A. S. Zibrov, M. Endres, M. Greiner *et al.*, Probing many-body dynamics on a 51-atom quantum simulator, Nature (London) **551**, 579 (2017).

[15] J. Zhang, G. Pagano, P. W. Hess, A. Kyprianidis, P. Becker, H. Kaplan, A. V. Gorshkov, Z.-X. Gong, and C. Monroe, Observation of a many-body dynamical phase transition with a 53-qubit quantum simulator, Nature (London) **551**, 601 (2017).

[16] C. Neill, P. Roushan, K. Kechedzhi, S. Boixo, S. V. Isakov, V. Smelyanskiy, A. Megrant, B. Chiaro, A. Dunsworth, K. Arya *et al.*, A blueprint for demonstrating quantum supremacy with superconducting qubits, Science **360**, 195 (2018).

[17] G. Brassard, P. Høyer, and M. Mosca, Quantum amplitude amplification and estimation, Quantum Comput. Quantum Inf. **305**, 53 (2002).

[18] I. L. Chuang, N. Gershenfeld, and M. Kubinec, Experimental Implementation of Fast Quantum Searching, Phys. Rev. Lett. **80**, 3408 (1998).

[19] C. Zalka, Grover's quantum searching algorithm is optimal, Phys. Rev. A **60**, 2746 (1999).

[20] D. S. Abrams and C. P. Williams, Fast quantum algorithms for numerical integrals and stochastic processes, arXiv:quant-ph/9908083.

[21] L. GuiLu, Z. WeiLin, L. YanSong, and N. Li, Arbitrary phase rotation of the marked state cannot be used for Grover's quantum search algorithm, Commun. Theor. Phys. **32**, 335 (1999).

[22] P. G. Kwiat, J. R. Mitchell, P. D. D. Schwindt, and A. G. White, Grover's search algorithm: An optical approach, J. Mod. Opt. **47**, 257 (2000).

[23] Z. Hao-Sheng and K. Le-Man, Preparation of GHZ states via Grover's quantum searching algorithm, Chin. Phys. Lett. **17**, 410 (2000).

[24] G. L. Long, Grover algorithm with zero theoretical failure rate, Phys. Rev. A **64**, 022307 (2001).

[25] E. Biham and D. Kenigsberg, Grover's quantum search algorithm for an arbitrary initial mixed state, Phys. Rev. A **66**, 062301 (2002).

[26] S. Heinrich, Quantum summation with an application to integration, J. Complex. **18**, 1 (2002).

[27] J. Roland and N. J. Cerf, Quantum-circuit model of Hamiltonian search algorithms, Phys. Rev. A **68**, 062311 (2003).

[28] L. Xiao and J. A. Jones, Error tolerance in an NMR implementation of Grover's fixed-point quantum search algorithm, Phys. Rev. A **72**, 032326 (2005).

[29] J. Jones, M. Mosca, and R. Hansen, Implementation of a quantum search algorithm on a quantum computer, Nature (London) **393**, 344 (1998).

[30] L. M. K. Vandersypen, M. Steffen, M. H. Sherwood, C. S. Yannoni, G. Breyta, and I. L. Chuang, Implementation of a three-quantum-bit search algorithm, Appl. Phys. Lett. **76**, 646 (2000).

[31] V. L. Ermakov and B. M. Fung, Experimental realization of a continuous version of the Grover algorithm, Phys. Rev. A **66**, 042310 (2002).

[32] N. Bhattacharya, H. B. van Linden van den Heuvell, and R. J. C. Spreeuw, Implementation of Quantum Search Algorithm using Classical Fourier Optics, Phys. Rev. Lett. **88**, 137901 (2002).

[33] Z. Jing-Fu, L. Zhi-Heng, D. Zhi-Wei, and S. Lu, NMR analogue of the generalized Grover's algorithm of multiple marked states and its application, Chin. Phys. **12**, 700 (2003).

[34] P. Walther, K. Resch, T. Rudolph, E. Schenck, H. Weinfurter, V. Vedral, M. Aspelmeyer, and A. Zeilinger, Experimental one-way quantum computing, Nature (London) **434**, 169 (2005).

[35] K.-A. Brickman, P. C. Haljan, P. J. Lee, M. Acton, L. Deslauriers, and C. Monroe, Implementation of Grover's quantum search algorithm in a scalable system, Phys. Rev. A **72**, 050306(R) (2005).

[36] L. DiCarlo, J. Chow, J. Gambetta, L. Bishop, B. Johnson, D. Schuster, J. Majer, A. Blais, L. Frunzio, S. Girvin, and R. Schoelkopf, Demonstration of two-qubit algorithms with a superconducting quantum processor, Nature (London) **460**, 240 (2009).

[37] C. Figgatt, D. Maslov, K. A. Landsman, N. M. Linke, S. Debnath, and C. Monroe, Complete 3-qubit Grover search on a programmable quantum computer, Nat. Commun. **8**, 1918 (2017).

[38] E. Bernstein and U. Vazirani, Quantum complexity theory, SIAM J. Comput. **26**, 1411 (1997).

[39] A. Bassi and D.-A. Deckert, Noise gates for decoherent quantum circuits, Phys. Rev. A **77**, 032323 (2008).

[40] J. Preskill, Course information for Physics 219/Computer Science 219 Quantum Computation, available at http://theory.caltech.edu/~preskill/ph229/ (2000).

[41] M. A. Nielsen and I. L. Chuang, *Quantum Computation and Quantum Information*, 10th ed. (Cambridge University Press, Cambridge, 2011).

[42] J. P. Barnes and W. S. Warren, Decoherence and programmable quantum computation, Phys. Rev. A **60**, 4363 (1999).

[43] B. Pablo-Norman and M. Ruiz-Altaba, Noise in Grover's quantum search algorithm, Phys. Rev. A **61**, 012301 (1999).

[44] H. Azuma, Decoherence in Grover's quantum algorithm: Perturbative approach, Phys. Rev. A **65**, 042311 (2002).

[45] G. L. Long, Y. S. Li, W. L. Zhang, and C. C. Tu, Dominant gate imperfection in Grover's quantum search algorithm, Phys. Rev. A **61**, 042305 (2000).

[46] J. Bae and Y. Kwon, Perturbations can enhance quantum search, Int. J. Theor. Phys. **42**, 2075 (2003).

[47] J. Chen, D. Kaszlikowski, L. Kwek, and C. Oh, Searching a database under decoherence, Phys. Lett. A **306**, 296 (2003).

[48] D. Shapira, S. Mozes, and O. Biham, Effect of unitary noise on Grover's quantum search algorithm, Phys. Rev. A **67**, 042301 (2003).

[49] P. Gawron, J. Klamka, and R. Winiarczyk, Noise effects in the quantum search algorithm from the viewpoint of computational complexity, Int. J. Appl. Math. Comput. Sci. **22**, 493 (2012).

[50] D. Reitzner and M. Hillery, Grover search under localized dephasing, Phys. Rev. A **99**, 012339 (2019).

[51] P. Salas, Noise effect on Grover algorithm, Eur. Phys. J. D **46**, 365 (2008).

[52] J. Hasegawa, Variety of effects of decoherence in quantum algorithms, IEICE Trans. Fund. Electron. Commun. Comput. Sci. **E92-A**, 1284 (2009).

[53] I. Cohn, A. L. F. De Oliveira, E. Buksman, and J. G. L. De Lacalle, Grover's search with local and total depolarizing channel errors: Complexity analysis, Int. J. Quantum Inf. **14**, 1650009 (2016).

[54] P. Vrana, D. Reeb, D. Reitzner, and M. Wolf, Fault-ignorant quantum search, New J. Phys. **16**, 073033 (2014).

[55] A. Steane, Multiple-particle interference and quantum error correction, Proc. R. Soc. A **452**, 2551 (1996).

[56] P. Botsinis, Z. Babar, D. Alanis, D. Chandra, H. Nguyen, S. X. Ng, and L. Hanzo, Quantum error correction protects quantum search algorithms against decoherence, Sci. Rep. **6**, 38095 (2016).

[57] R. Alicki, M. Horodecki, P. Horodecki, and R. Horodecki, Dynamical description of quantum computing: Generic non-locality of quantum noise, Phys. Rev. A **65**, 062101 (2002).

[58] R. C. Bialczak, R. McDermott, M. Ansmann, M. Hofheinz, N. Katz, E. Lucero, M. Neeley, A. D. O'Connell, H. Wang, A. N.

Cleland, and J. M. Martinis, $1/f$ Flux Noise in Josephson Phase Qubits, Phys. Rev. Lett. **99**, 187006 (2007).

[59] J. Bylander, S. Gustavsson, F. Yan, F. Yoshihara, K. Harrabi, G. Fitch, D. G. Cory, Y. Nakamura, J.-S. Tsai, and W. D. Oliver, Noise spectroscopy through dynamical decoupling with a superconducting flux qubit, Nat. Phys. **7**, 565 (2011).

[60] E. Paladino, Y. M. Galperin, G. Falci, and B. L. Altshuler, $1/f$ noise: Implications for solid-state quantum information, Rev. Mod. Phys. **86**, 361 (2014).

[61] S. Bose, Quantum Communication through an Unmodulated Spin Chain, Phys. Rev. Lett. **91**, 207901 (2003).

[62] F. Haake, *Quantum Statistics in Optics and Solid-State Physics*, Springer Tracts in Modern Physics (Springer, Berlin, 1973), Vol. 66.

[63] S. Daffer, K. Wódkiewicz, J. D. Cresser, and J. K. McIver, Depolarizing channel as a completely positive map with memory, Phys. Rev. A **70**, 010304(R) (2004).

[64] S. Maniscalco and F. Petruccione, Non-Markovian dynamics of a qubit, Phys. Rev. A **73**, 012111 (2006).

[65] F. Buscemi and P. Bordone, Time evolution of tripartite quantum discord and entanglement under local and nonlocal random telegraph noise, Phys. Rev. A **87**, 042310 (2013).

[66] M. M. Ali, P.-Y. Lo, and W.-M. Zhang, Exact decoherence dynamics of $1/f$ noise, New J. Phys. **16**, 103010 (2014).

[67] C. Benedetti, M. G. A. Paris, and S. Maniscalco, Non-Markovianity of colored noisy channels, Phys. Rev. A **89**, 012114 (2014).

[68] C. Addis, G. Karpat, C. Macchiavello, and S. Maniscalco, Dynamical memory effects in correlated quantum channels, Phys. Rev. A **94**, 032121 (2016).

[69] K. Schultz, G. Quiroz, P. Titum, and B. D. Clader, SchWARMA: A model-based approach for time-correlated noise in quantum circuits, Phys. Rev. Res. **3**, 033229 (2021).

[70] R. Harper, S. T. Flammia, and J. J. Wallman, Efficient learning of quantum noise, Nat. Phys. **16**, 1184 (2020).

[71] P. Aliferis, D. Gottesman, and J. Preskill, Quantum accuracy threshold for concatenated distance-3 code, Quantum Inf. Comput. **6**, 97 (2006).

[72] D. Aharonov, A. Kitaev, and J. Preskill, Fault-Tolerant Quantum Computation with Long-Range Correlated Noise, Phys. Rev. Lett. **96**, 050504 (2006).

[73] J. P. Clemens, S. Siddiqui, and J. Gea-Banacloche, Quantum error correction against correlated noise, Phys. Rev. A **69**, 062313 (2004).

[74] R. Klesse and S. Frank, Quantum Error Correction in Spatially Correlated Quantum Noise, Phys. Rev. Lett. **95**, 230503 (2005).

[75] E. Novais, E. R. Mucciolo, and H. U. Baranger, Hamiltonian formulation of quantum error correction and correlated noise: Effects of syndrome extraction in the long-time limit, Phys. Rev. A **78**, 012314 (2008).

[76] C. Cafaro and S. Mancini, Quantum stabilizer codes for correlated and asymmetric depolarizing errors, Phys. Rev. A **82**, 012306 (2010).

[77] B. D. Clader, C. J. Trout, J. P. Barnes, K. Schultz, G. Quiroz, and P. Titum, Impact of correlations and heavy tails on quantum error correction, Phys. Rev. A **103**, 052428 (2021).

[78] C. Macchiavello and G. M. Palma, Entanglement-enhanced information transmission over a quantum channel with correlated noise, Phys. Rev. A **65**, 050301(R) (2002).

[79] C. Macchiavello, G. M. Palma, and S. Virmani, Transition behavior in the channel capacity of two-qubit channels with memory, Phys. Rev. A **69**, 010303(R) (2004).

[80] D. Daems, Entanglement-enhanced transmission of classical information in Pauli channels with memory: Exact solution, Phys. Rev. A **76**, 012310 (2007).

[81] A. Y. Kitaev, A. H. Shen, and M. N. Vyalyi, *Classical and Quantum Computation* (American Mathematical Society, Providence, 2002).

[82] J. Preskill, Quantum Computing in the NISQ era and beyond, Quantum **2**, 79 (2018).

[83] P. Murali, N. M. Linke, M. Martonosi, A. J. Abhari, N. H. Nguyen, and C. H. Alderete, in *Proceedings of the 2019 ACM/IEEE 46th Annual International Symposium on Computer Architecture (ISCA)* (IEEE, Piscataway, 2019), pp. 527–540.

[84] D. Kwiatkowski and L. Cywiński, Decoherence of two entangled spin qubits coupled to an interacting sparse nuclear spin bath: Application to nitrogen vacancy centers, Phys. Rev. B **98**, 155202 (2018).

[85] U. von Lüpke, F. Beaudoin, L. M. Norris, Y. Sung, R. Winik, J. Y. Qiu, M. Kjaergaard, D. Kim, J. Yoder, S. Gustavsson, L. Viola, and W. D. Oliver, Two-qubit spectroscopy of spatiotemporally correlated quantum noise in superconducting qubits, PRX Quantum **1**, 010305 (2020).

[86] J. M. Gambetta, A. D. Córcoles, S. T. Merkel, B. R. Johnson, J. A. Smolin, J. M. Chow, C. A. Ryan, C. Rigetti, S. Poletto, T. A. Ohki, M. B. Ketchen, and M. Steffen, Characterization of Addressability by Simultaneous Randomized Benchmarking, Phys. Rev. Lett. **109**, 240504 (2012).

[87] T. J. Proctor, A. Carignan-Dugas, K. Rudinger, E. Nielsen, R. Blume-Kohout, and K. Young, Direct Randomized Benchmarking for Multiqubit Devices, Phys. Rev. Lett. **123**, 030503 (2019).

[88] M. Sarovar, T. Proctor, K. Rudinger, K. Young, E. Nielsen, and R. Blume-Kohout, Detecting crosstalk errors in quantum information processors, Quantum **4**, 321 (2020).

[89] P. Murali, D. C. McKay, M. Martonosi, and A. Javadi-Abhari, in *Proceedings of the Twenty-Fifth International Conference on Architectural Support for Programming Languages and Operating Systems* (ACM, New York, 2020), pp. 1001–1016.

[90] P. Zhao, K. Linghu, Z. Li, P. Xu, R. Wang, G. Xue, Y. Jin, and H. Yu, Quantum crosstalk analysis for simultaneous gate operations on superconducting qubits, PRX Quantum **3**, 020301 (2022).

[91] H. Klauck, in *Proceedings of the Thirty-Fifth Annual ACM Symposium on Theory of Computing* (Association for Computing Machinery, New York, 2003), pp. 69–76.

[92] S. Sinha and P. Russer, Quantum computing algorithm for electromagnetic field simulation, Quantum Inf. Process. **9**, 385 (2010).

[93] A. Barenco, C. H. Bennett, R. Cleve, D. P. DiVincenzo, N. Margolus, P. Shor, T. Sleator, J. A. Smolin, and H. Weinfurter, Elementary gates for quantum computation, Phys. Rev. A **52**, 3457 (1995).

[94] D. P. L. A. Craik, N. M. Linke, M. A. Sepiol, T. P. Harty, J. F. Goodwin, C. J. Ballance, D. N. Stacey, A. M. Steane, D. M. Lucas, and D. T. C. Allcock, High-fidelity spatial and polarization addressing of $^{43}Ca^+$ qubits using near-field microwave control, Phys. Rev. A **95**, 022337 (2017).

[95] A. Erhard, J. J. Wallman, L. Postler, M. Meth, R. Stricker, E. A. Martinez, P. Schindler, T. Monz, J. Emerson, and R. Blatt, Characterizing large-scale quantum computers via cycle benchmarking, Nat. Commun. **10**, 5347 (2019).

[96] B. Lienhard, J. Braumüller, W. Woods, D. Rosenberg, G. Calusine, S. Weber, A. Vepsäläinen, K. O'Brien, T. P. Orlando, S. Gustavsson, and W. D. Oliver, in *Proceedings of the 2019 IEEE MTT-S International Microwave Symposium (IMS)* (IEEE, Piscataway, 2019), pp. 275–278.

[97] P. Murali, J. M. Baker, A. Javadi-Abhari, F. T. Chong, and M. Martonosi, in *Proceedings of the Twenty-Fourth International Conference on Architectural Support for Programming Languages and Operating Systems* (Association for Computing Machinery, New York, 2019), pp. 1015–1029.

[98] A. Molavi, A. Xu, M. Diges, L. Pick, S. Tannu, and A. Albarghouthi, in *Proceedings of the 2022 55th IEEE/ACM International Symposium on Microarchitecture (MICRO)* (IEEE, Piscataway, 2022), pp. 1078–1091.

[99] L. Chhangte and A. Chakrabarty, Near-optimal circuit mapping with reduced search paths on IBM quantum architectures, Microprocess. Microsyst. **94**, 104637 (2022).

[100] L. Burgholzer, S. Schneider, and R. Wille, in *Proceedings of the 2022 27th Asia and South Pacific Design Automation Conference (ASP-DAC)* (IEEE, Piscataway, 2022), pp. 466–471.

[101] E. Onorati, O. Buerschaper, M. Kliesch, W. Brown, A. H. Werner, and J. Eisert, Mixing properties of stochastic quantum Hamiltonians, Commun. Math. Phys. **355**, 905 (2017).

[102] A. Blais, R.-S. Huang, A. Wallraff, S. M. Girvin, and R. J. Schoelkopf, Cavity quantum electrodynamics for superconducting electrical circuits: An architecture for quantum computation, Phys. Rev. A **69**, 062320 (2004).

[103] C. E. Bradley, J. Randall, M. H. Abobeih, R. C. Berrevoets, M. J. Degen, M. A. Bakker, M. Markham, D. J. Twitchen, and T. H. Taminiau, A Ten-Qubit Solid-State Spin Register with Quantum Memory up to One Minute, Phys. Rev. X **9**, 031045 (2019).

[104] C. H. Bennett, Logical reversibility of computation, IBM J. Res. Dev. **17**, 525 (1973).

[105] S. Aaronson, Quantum lower bound for recursive fourier sampling, Quantum Inf. Comput. **3**, 165 (2003).

[106] M. Amy and N. J. Ross, Phase-state duality in reversible circuit design, Phys. Rev. A **104**, 052602 (2021).

[107] A. Paradis, B. Bichsel, S. Steffen, and M. Vechev, in *Proceedings of the 42nd ACM SIGPLAN International Conference on Programming Language Design and Implementation* (Association for Computing Machinery, New York, 2021), pp. 222–236.

[108] J. Doob, *Stochastic Processes* (Wiley, New York, 1953).

[109] J. G. Kemeny and J. L. Snell, *Finite Markov Chains* (Van Nostrand, Princeton, 1960).

[110] G. Grimmett and D. Stirzaker, *Probability and Random Processes* (Oxford University Press, Oxford, 2020).

[111] I. Bena, Dichotomous Markov noise: Exact results for out-of-equilibrium systems, Int. J. Mod. Phys. B **20**, 2825 (2006).

[112] T. Yu and J. Eberly, Sudden death of entanglement: Classical noise effects, Opt. Commun. **264**, 393 (2006).

[113] P. Szańkowski, M. Trippenbach, Ł. Cywiński, and Y. B. Band, The dynamics of two entangled qubits exposed to classical noise: Role of spatial and temporal noise correlations, Quantum Inf. Process. **14**, 3367 (2015).

[114] L. Aolita, F. De Melo, and L. Davidovich, Open-system dynamics of entanglement: A key issues review, Rep. Prog. Phys. **78**, 042001 (2015).

[115] P. Jurcevic and L. C. G. Govia, Effective qubit dephasing induced by spectator-qubit relaxation, Quantum Sci. Technol. **7**, 045033 (2022).

[116] K. Rudinger, T. Proctor, D. Langharst, M. Sarovar, K. Young, and R. Blume-Kohout, Probing Context-Dependent Errors in Quantum Processors, Phys. Rev. X **9**, 021045 (2019).

[117] G. Bowen and S. Mancini, Quantum channels with a finite memory, Phys. Rev. A **69**, 012306 (2004).

[118] H. P. Specht, C. Nölleke, A. Reiserer, M. Uphoff, E. Figueroa, S. Ritter, and G. Rempe, A single-atom quantum memory, Nature (London) **473**, 190 (2011).

[119] N. P. Kumar, S. Banerjee, R. Srikanth, V. Jagadish, and F. Petruccione, Non-Markovian evolution: A quantum walk perspective, Open Syst. Inf. Dyn. **25**, 1850014 (2018).

[120] D. Kretschmann and R. F. Werner, Quantum channels with memory, Phys. Rev. A **72**, 062323 (2005).

[121] F. Caruso, V. Giovannetti, C. Lupo, and S. Mancini, Quantum channels and memory effects, Rev. Mod. Phys. **86**, 1203 (2014).

[122] E. Sudarshan, P. Mathews, and J. Rau, Stochastic dynamics of quantum-mechanical systems, Phys. Rev. **121**, 920 (1961).

[123] M.-D. Choi, Completely positive linear maps on complex matrices, Linear Algebra Appl. **10**, 285 (1975).

[124] G. Lindblad, On the generators of quantum dynamical semigroups, Commun. Math. Phys. **48**, 119 (1976).

[125] K. Kraus, A. Böhm, J. D. Dollard, and W. Wootters, in *States, Effects, and Operations: Fundamental Notions of Quantum Theory*, edited by H. Araki, J. Ehlers, K. Hepp, R. Kippenhahn, H. A. Weidenmüller, and J. Zittartz, Lectures Notes in Physics (Springer, Berlin, 1983), Vol. 190.

[126] C. B. Mendl and M. M. Wolf, Unital quantum channels—convex structure and revivals of Birkhoff's Theorem, Commun. Math. Phys. **289**, 1057 (2009).